Influence of Spurious Modes on the Efficiency of Piezoelectric Transformers: A Sensitivity Analysis

Jack Forrester, Jonathan Neil Davidson, Martin P. Foster, and David A. Stone

***Abstract*—An analysis of the efficiency degradation resulting from spurious modes in piezoelectric transformers (PTs) is presented in this article. Circuit analysis is performed on PT equivalent circuit models with both a single resonant branch and with two resonant branches (spurious mode included), allowing the efficiency degradation from a spurious mode to be analyzed. Multiple sensitivity analyses were then performed, highlighting frequency difference (between modes) and characteristic impedance of the spurious resonant circuit ($\sqrt{L_2/C_2}$) as critical design parameters for minimizing efficiency degradation from spurious modes. These two parameters are further analyzed to determine optimum design conditions to ensure minimal efficiency degradation. Results of this analysis provide a method of estimating whether a spurious mode will degrade efficiency and consequently provide a method for improving PT designs.**

***Index Terms*—Converters, piezoelectric devices, sensitivity, transformers.**

I. Introduction

PIEZOELECTRIC transformers (PTs) are an alternative to traditional magnetic transformers. PTs are an assembly of one or more piezoelectric elements and make use of both the direct and converse piezoelectric effects to transform electrical energy. High power density, low electromagnetic interference and the absence of magnetic fields are some of the advantages PTs offer over their magnetic counterparts. PTs are resonant devices and so are ideal for use in resonant converter and related power electronics applications [1]–[5]. One of the interesting properties of PTs is the large quality factor they exhibit—this typically leads to minimal losses and so, as a result, PT and PT-based converters can achieve high electrical efficiency [6].

PTs exhibit and consequently can be operated with a wide variety of different vibration shapes (modes), as shown in Fig. 1, with the longitudinal, planar, and thickness modes being most common. Each PT can exhibit many of the possible vibration modes, each occurring at a different frequency. However, each PT topology has an optimum vibration mode that will allow optimum energy transfer through the device. The optimum vibration mode for a PT will typically be the mode that exhibits the highest electromechanical coupling and has the lowest losses, as can be observed by the 120-kHz mode occurring in Fig. 1. Therefore, it is also the mode that exhibits the highest output power and efficiency. As a result, designers will often optimize a PT design exclusively for optimum mode performance.

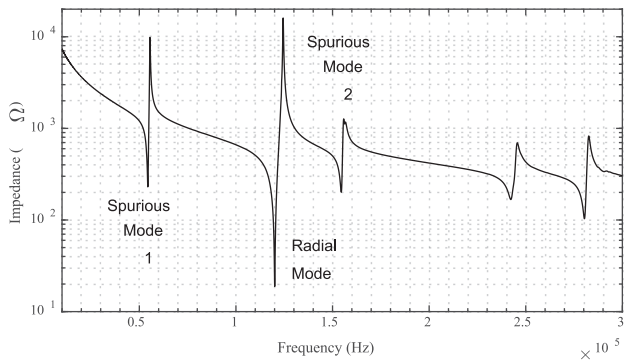

Fig. 1. Impedance spectrum of the T1-13 radial mode Transoner PT; radial mode is exhibited at 120 kHz.

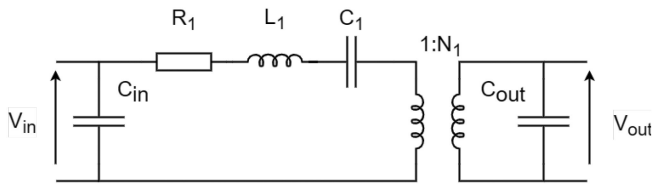

Fig. 2. Mason equivalent circuit model of a PT.

The Mason equivalent circuit model (see Fig. 2) can be used to model the electrical behavior of the optimum mode, of any topology or type of PT and, importantly, it allows the use of circuit analysis techniques on PTs. It should be noted that the model used here is a simplified Mason equivalent circuit; the full model contains two ideal transformers at the input and output. The full model is not necessary for the analysis in this article. The individual components of the equivalent circuit are linked to the physical properties of the PT. Output and input capacitances model the parallel electrodes of the PT and the ideal transformer models the transfer of energy from the electrical input to the mechanical vibration and, finally, to the electrical output. The *RLC* section models the resonant behavior of the PT and, whereas the input and output capacitances exist electrically, the *RLC* section models purely mechanical behavior.

Manuscript received December 20, 2019; revised April 4, 2020; accepted May 26, 2020. Date of publication June 9, 2020; date of current version September 4, 2020. This work was supported by the Engineering and Physical Sciences Research Council under Grant EP/P015859/1. Recommended for publication by Associate Editor Q. Li. *(Corresponding author: Jonathan Neil Davidson.)*

The authors are with the Department of Electronic and Electrical Engineering, University of Sheffield, Sheffield S1 3JD, U.K. (e-mail: jforrester1@sheffield.ac.uk; jonathan.davidson@sheffield.ac.uk; M.P.Foster@sheffield.ac.uk; D.A.Stone@sheffield.ac.uk).

Color versions of one or more of the figures in this article are available online at https://ieeexplore.ieee.org.

Digital Object Identifier 10.1109/TPEL.2020.3001486

Forrester *et al.* [7] described a process for designing a radial mode Transoner PT. Initially, the turns ratio is selected based on the input voltage and desired output voltage, giving the number of layers. Then, layer thicknesses are optimized to ensure zero voltage switching (ZVS) is achieved when used as part of a half-bridge-based inductor-less resonant converter [8]. Finally, the radius and total thickness are designed given the available disc sizes, desired resonant frequency, and required output power [9]. The resulting transformer is then suitably designed for operation at the optimum mode.

However, the remaining nonoptimum (spurious) vibration modes can interfere with the optimum mode of the PT, reducing the lifetime of the device and its energy transfer efficiency [10]. Therefore, one of the challenges PT designers must contend with is designing the PT in such a way as to limit the influence of these modes while not affecting optimum mode performance.

Researchers take a variety of approaches to avoid these interactions. One of the most popular methods for avoiding interference from spurious modes is by careful selection of the piezoelectric material used. Ohnishi *et al.* [11] created a thickness mode PT using lead titanate. A thickness mode PT would typically have to contend with spurious longitudinal vibrations influencing the performance of the PT. One of the key features of lead titanate is that it exhibits a K_t coupling factor much greater than the K_{31} coupling factor. The coupling factor describes the ratio of stored mechanical energy to supplied electric energy [12]. Therefore, in a PT made from this material, spurious longitudinal vibrations (those in the 31 directions) transfer less energy compared to thickness (t-direction) vibrations. Similarly, Prieto *et al.* [13] also proposed using lead titanate for reducing the effect of spurious modes. However, they found that the resulting devices had lower electromechanical coupling in the optimum vibration mode than those made from traditional lead zirconium titanate (PZT) materials and therefore had reduced power density. To overcome the limitation, Prieto *et al.* proposed altering the shape of the PT, including adding a hole in the center of the device to reduce unwanted vibrations for PZT-based devices; however, their method requires careful design and appropriate mounting to avoid damping the vibration. Sanz *et al.* [14] used interleaved electrodes to create a symmetrically designed Rosen PT. Although this method shows some good results, it is only applicable to certain topologies and, even then, reduces the design space for those topologies.

While these efforts have reduced the impact of spurious modes, they require sacrificing device performance and, while they reduce the overall effect of spurious modes, these modes are not eliminated. Our approach in this article, rather than attempting to eliminate spurious modes, is to design the PT in such a way that spurious modes have negligible effect on performance, without affecting optimum mode performance. The analysis will be aimed at giving a PT designer the information required, given some knowledge of the equivalent circuit of the PT, to determine whether a PT will exhibit minimal efficiency loss from spurious modes. The analysis will identify which design element or feature needs to change for the PT to achieve minimal interference from spurious modes.

For this analysis, the Mason equivalent circuit model of the PT is used, allowing the results of the analysis to be applicable to all PT topologies. This article will form part of a wider framework that explores the optimum geometric/material design of specific PT topologies for minimal spurious mode interaction, based on the results of the analysis presented here. Initially, the efficiency of the idealized single-mode PT is analyzed and the elements of its equivalent circuit that influence this efficiency are determined. The equivalent circuit model of the PT is then extended to include another resonant element (i.e., a spurious mode) and the modified efficiency of this equivalent circuit is examined. This allows the efficiency degradation from the interaction between the optimum and spurious modes, when the PT is driven at the optimum (operating) mode, to be analyzed through multiple sensitivity analyses. Using the results of this analysis, the key factors that affect the efficiency degradation are highlighted. Further, quantitative restrictions on the design space, in terms of equivalent circuit parameter values, are proposed. Observing this restriction will result in minimal degradation in efficiency for each specific PT. Finally, the results are verified by experimental measurements.

II. Impact of PT Design on Efficiency Loss From Spurious Modes

First, increased frequency separation between optimum and spurious modes will be analyzed for its impact on efficiency, using a COMSOL simulation. Then, the analysis will be performed using ac circuit analysis techniques on simplified and extended Mason equivalent circuit models. Using the mathematical models generated for efficiency, an expression for the efficiency degradation from spurious modes can be found, allowing sensitivity analyses to be performed, highlighting key parameters for minimizing efficiency degradation.

A. Spurious Mode Proximity to Optimum Mode

This section analyzes the impact proximity of modes has on the overall efficiency of the PT. Maximizing the frequency separation between operating and spurious modes is the most obvious method for minimizing interaction between modes. Spurious mode frequencies are generally influenced by changing the dimensions of a device, for example, controlling the radius/thickness ratio of a radial mode Transoner PT controls the spurious mode resonant frequencies. Intuitively, and correctly, the greater the separation in the frequency of the optimum and the spurious modes, the lesser the effect the spurious mode has on efficiency.

A COMSOL simulation was used to validate this assumption. A 2-D axisymmetric, two-layer radial mode Transoner PT (see Fig. 3) model is created in COMSOL. The radius of the PT is varied from 5 to 15 mm and the thickness of the PT (t) is varied from 1 to 5 mm. The two layers are equal in thickness ($t_1 = t_2$), the PTs are made from PZT4 and the Q-factor of the optimum mode is fixed at 150. For each PT studied the efficiency of the PT is determined at the optimum mode resonant frequency. A sinusoidal input voltage and a matched load are

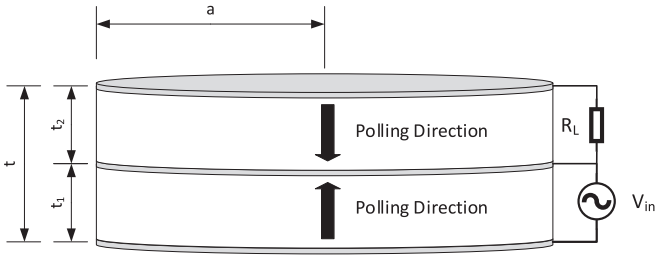

Fig. 3. Two-layer radial mode Transoner PT.

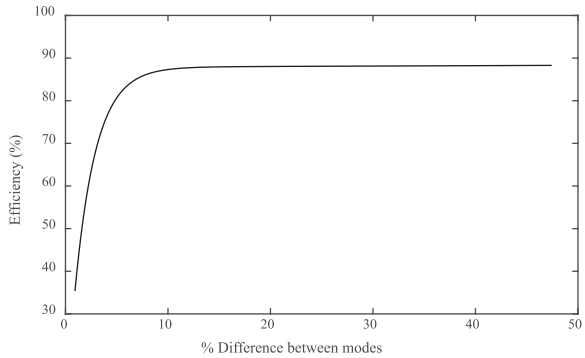

Fig. 4. Exponential line of best fit for the simulated efficiency of multiple PT models from COMSOL against percentage difference between optimum and nearest spurious mode resonant frequencies.

used. The resonant frequency of the closest spurious mode is also extracted. The resulting efficiencies are plotted against the percentage difference in frequency between the ideal and spurious modes. The results of this are shown in Fig. 4.

With increased frequency difference, higher efficiencies tend to be achieved (but there are exceptions). However, achieving a large frequency difference between optimum and spurious modes requires careful control of the PT dimensions and therefore limits the PT design space. As the frequency difference between the ideal and a spurious mode increases, the ideal mode might move to a frequency closer to that of another spurious mode because a PT can exhibit multiple spurious modes. Therefore, designing the PT to exhibit very large frequency difference between the optimum and one particular spurious mode is unlikely to result in an optimized design.

It is also likely that other design criteria will affect the frequency difference required to achieve a desired level of efficiency. Therefore, these other elements will be analyzed.

B. Efficiency Modeling

To analyze these design elements, the Mason equivalent circuit model will be used. First, the single-branch Mason equivalent circuit model will be used to analyze the efficiency of an idealized single-mode PT (η_1)—this is an imagined PT with all spurious modes deleted. The Mason model will then be extended to include multiple resonant branches, allowing both operating and spurious modes to be modeled together. This allows the efficiency of a PT, driven at the optimum mode resonant frequency and including the effects of a spurious mode, to be analyzed (η_2). Finally, a metric describing the loss in efficiency originating from the spurious mode $(\Delta\eta)$ will be found.

1) Efficiency in the Single-Branch Model (η_1)*:* It is well known that PTs can achieve high efficiency due to the high *Q*-factor exhibited by the hard piezoelectric materials employed in their construction. The efficiency ratio η_1 of a device is defined as follows:

$$\eta_1(\omega) = \frac{P_{\text{out}}(\omega)}{P_{\text{in}}(\omega)}. \tag{1}$$

By generating equations for the voltage and currents in the device, equations for the input and output power can be found. The input and output currents can be written, in the frequency domain, as

$$I_{\text{in}}(\omega) = \frac{V_{\text{in}} - \frac{V_{\text{out}}(\omega)}{N_1}}{R_1 + jX_1} + j\omega C_{\text{in}} V_{\text{in}} \tag{2}$$

$$I_{\text{out}}(\omega) = \frac{V_{\text{out}}(\omega)}{R_L} \tag{3}$$

where X_1 is the reactance of the *LC* branch

$$X_1 = \omega L_1 - \frac{1}{\omega C_1} \tag{4}$$

which allows V_{out} to be calculated as

$$V_{\text{out}}(\omega) = \frac{N_1 V_{\text{in}}}{1 + (R_1 + jX_1) N_1^2 \left(\frac{1}{R_L} - \frac{\text{j}}{X_{\text{out}}}\right)} \tag{5}$$

where X_{out} is the reactance of capacitor C_{out}. Power in and out can then be calculated. Note that the input capacitor dissipates no power. Together with the output power, an expression for efficiency can be derived. Producing the full solution is trivial with computer algebra packages such as Maple but excessively long to present and is therefore omitted

$$P_{\text{in}}(\omega) = \Re\left(V_{\text{in}}(\omega) I_{\text{in}}(\omega)^*\right) = \Re\left(\frac{V_{\text{in}}^2 - \frac{V_{\text{in}} V_{\text{out}}(\omega)}{N_1}}{R_1 + jX_1}\right) \tag{6}$$

$$P_{\text{out}}(\omega) = \frac{|V_{\text{out}}(\omega)|^2}{R_L}. \tag{7}$$

By combining all these equations, it can be shown that

$$\eta_1(\omega) = \frac{R_L}{R_1\left(\omega^2 {C_{\text{out}}}^2 {R_L}^2 + 1\right) N_1^2 + R_L}. \tag{8}$$

Equation (8) suggests there are several equivalent circuit elements that ought to be carefully selected to achieve high efficiency. The damping resistance (R_1) has a significant effect on efficiency (from heat dissipation modeled as I^2R losses). However, R_1 is multiplied by $\omega^2 {C_{\text{out}}}^2 {R_L}^2$ and N_1^2, therefore higher efficiency operation is achieved for low values of all these parameters. However, C_{out} should be carefully designed to ensure ZVS can be achieved, as shown by Foster *et al.* [8], and N will be chosen depending on the required application of the PT. Due to the implications of minimizing C_{out} and N,

TABLE I
T1-13 RADIAL MODE PT EQUIVALENT CIRCUIT PARAMETERS, INCLUDING OPTIMAL AND CLOSEST OCCURRING SPURIOUS MODE

R_1	R_2	L_1	L_2	C_1
18.9 Ω	233.7 Ω	12.7 mH	95.2 mH	138.7 pF
C_2	N_1	N_2	C_{in}	C_{out}
89.8 pF	0.88	1.32	1.90 nF	1.21 nF

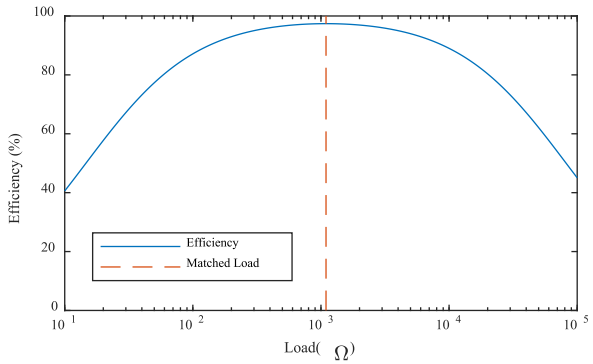

Fig. 5. Efficiency of the single-branch equivalent circuit model of the T1-13 radial mode PT against load.

it is advantageous to ensure R_1 is minimized as this has no detrimental effects.

To ensure optimal efficiency, the load is often matched to the output capacitance as shown in the following equation [15]:

$$R_L = \frac{1}{\omega C_{\text{out}}} \tag{9}$$

and hence (8) can be simplified to

$$\eta_1(\omega) = \frac{1}{2N_1^2 \omega C_{\text{out}} R_1 + 1}. \tag{10}$$

To analyze the effect of using an unmatched load on the efficiency of the PT, the efficiency of the single-branch model can be simulated under various load conditions. Equation (8) was used with the equivalent circuit parameters for the optimum mode of the T1-13 Transoner PT defined in Table I, and assuming the PT was driven at the series resonant frequency. The resulting efficiency against load curve is shown in Fig. 5.

As can be seen in Fig. 5, η_1 peaks when the load is equal to the matched load. Very small or very large loads should be avoided as this gives low efficiency. When R_L is small, the output voltage is low and therefore the voltage across the resonant circuit is maximized, increasing I^2R losses. When R_L is large, the output current is much lower than the current through the resonant circuit, again lowering the efficiency. Also from (10), it can be seen that the matched load is dependent on frequency, which adds to the complexity of designing and controlling PT-based power converters.

2) Multiple Branch Model: The model shown in Fig. 2 is a simplification of the full equivalent circuit and, as a result, is only applicable when the PT is driven at the resonant frequency of the optimum mode and when all other vibration modes have negligible effect. The full equivalent circuit model of a PT contains

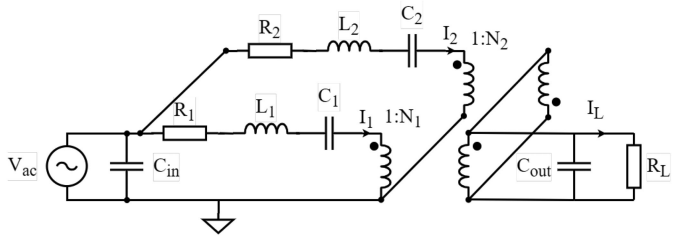

Fig. 6. Extended Mason equivalent circuit model of a PT.

many *RLC* branches, which model each of the different vibration modes. Lin [16] showed that each of these *RLC* branches should be connected to the output node of the PT through an ideal transformer to correctly model the impedance and performance of a PT, as shown in Fig. 6. Although the PT contains many vibration modes, most of these have high impedance at the operating frequency and pass negligible current, and thus have negligible influence on the performance of the PT. They can therefore be omitted from the model. However, even when considering a small number of spurious modes, the analysis on the efficiency of the PT is difficult. As a result, the investigation in this article will consider only two modes interacting: the optimum mode and a single spurious mode.

a) Efficiency in the multiple branch model (η_2): An understanding of the efficiency loss mechanism in the multiple branch model is required before analyzing the impact of a spurious mode on efficiency. To begin, a frequency domain analysis was performed using the equivalent circuit model in Fig. 6 and the equivalent circuit parameters of a T1-13 radial mode Transoner PT (see Table I). The efficiency suggested by the model was examined and shown in Fig. 7.

As can be observed in Fig. 7, while the efficiency is usually high around the optimum mode, there is a region of significant inefficiency near the spurious mode resonant frequency. This effect is due to the interaction between the two resonant modes. To understand the reason for this interaction, the current through the resonant branches, when the PT is operated at the minimum efficiency frequency (∼43 kHz in Fig. 7), is analyzed and is shown in Fig. 8, where I_1, I_2, and I_L are the currents through the optimum mode branch, spurious mode branch, and the load, respectively.

The resonant branch currents are near-equal in magnitude and in antiphase and when combined through the transformer, this results in negligible output current. Energy loss is incurred through damping: there is still notable input power. There is a large region of frequencies where this interaction occurs and degrades the efficiency. In this region, the currents suffer destructive interference. It should be noted that other factors, such as the load, have an impact on the range of frequencies that are affected by the efficiency loss as demonstrated by the different curve shapes shown in Fig. 7.

To minimize the effect of spurious modes on the efficiency of a PT, the condition where there is significant interference should be avoided or should occur at frequencies away from the optimum mode, where the power transfer is

TABLE II
EQUIVALENT CIRCUIT PARAMETERS FOR THE T1-13 PT AND THE ADJUSTED T1-13 PT, TERMED THE T1*

	R_1	R_2	$\omega_1/2\pi$	$\omega_2/2\pi$	ζ_1	ζ_2	N_1	N_2	C_{in}	C_{out}
T1-13	18.9 Ω	233.7 Ω	120.1 kHz	54.4 kHz	9556.3 Ω	32568 Ω	0.88	1.32	1.90 nF	1.21 nF
T1*	18.9 Ω	233.7 Ω	120.1 kHz	108.3 kHz	9556.3 Ω	32568 Ω	0.88	1.32	1.90 nF	1.21 nF

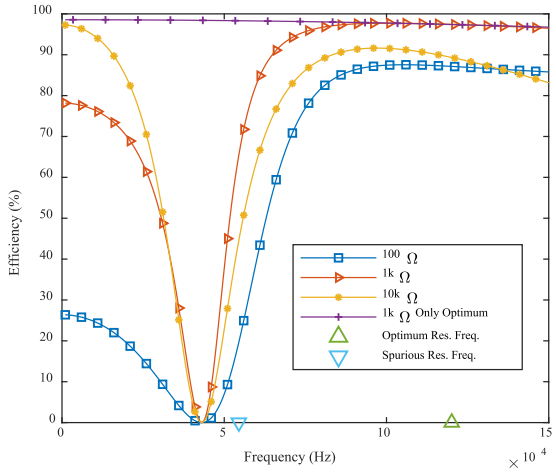

Fig. 7. Efficiency of a two-branch equivalent circuit model of the T1-13 PT against operating frequency under various load conditions, single-branch efficiency included for 1-kΩ load for comparison.

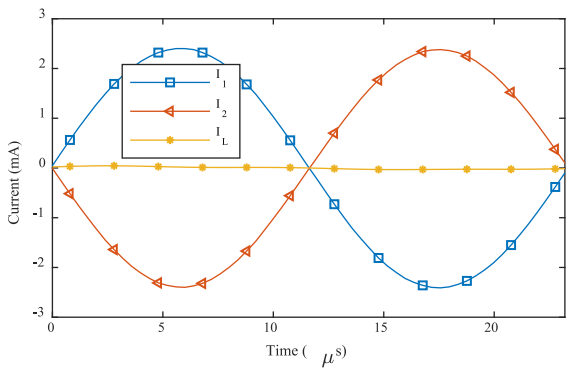

Fig. 8. Current flowing through the optimum mode, spurious mode, and load at 43 kHz.

already negligible. As shown in Fig. 4, increasing the frequency difference between modes helps to ensure high efficiency because the minimum efficiency frequency would then occur away from the optimum mode. Also, the range of frequencies at which destructive interference occurs should be minimized.

b) Efficiency modeling for two modes: To determine the best method of minimizing spurious mode influence on efficiency, it is first necessary to derive an expression of the efficiency of a PT containing an ideal and a spurious vibration mode.

To determine the efficiency of the circuit in Fig. 6, when operated at the optimum mode resonant frequency, an equation for the input and output power is derived in terms of the equivalent circuit component values. The power and efficiency can be derived by considering the current in each resonant branch and the output current in terms of input and output voltages

$$I_1(\omega) = \frac{V_{\text{in}} - \frac{V_{\text{out}}(\omega)}{N_1}}{R_1 + jX_1} \tag{11}$$

$$I_2(\omega) = \frac{V_{\text{in}} + \frac{V_{\text{out}}(\omega)}{N_2}}{R_2 + jX_2} \tag{12}$$

$$I_{\text{in}}(\omega) = I_1 + I_2 + j\omega C_{\text{in}} V_{\text{in}} \tag{13}$$

$$I_{\text{out}}(\omega) = \frac{V_{\text{out}}(\omega)}{R_L} \tag{14}$$

where X_1 and X_2 are the reactances of the *LC* combinations of branches 1 and 2, respectively. That is to say

$$X_n = \omega L_n - \frac{1}{\omega C_n}. \tag{15}$$

Assuming only these two branches are significant, (11), (12), and (14) can be rearranged to give an expression for V_{out}

$$V_{\text{out}}(\omega) = \frac{\frac{V_{\text{in}}}{(R_1+jX_1)N_1} + \frac{V_{\text{in}}}{(R_2+jX_2)N_2}}{\frac{1}{N_1^2(R_1+jX_1)} + \frac{1}{N_2^2(R_2+jX_2)} + \frac{1}{R_L} - \frac{j}{X_{\text{out}}}} \tag{16}$$

$$P_{\text{out}}(\omega) = \frac{|V_{\text{out}}(\omega)|^2}{R_L} \tag{17}$$

$$\eta_2(\omega) = \frac{P_{\text{out}}(\omega)}{P_{\text{in}}(\omega)} = \frac{P_{\text{out}}(\omega)}{\Re\left(V_{\text{in}}(\omega)\, I_{\text{in}}(\omega)^*\right)}. \tag{18}$$

A closed-form expression for η_2 can be easily derived by solving (11)–(13) and (16)–(18), but it is too long to print here. Instead, we will write η_2 in function format

$$\eta_2 = f(L_1,\ L_2,\ C_1,\ C_2,\ R_1,\ R_2,\ N_1,\ N_2,\ C_{\text{out}},\ \omega, R_L)\ . \tag{19}$$

3) Efficiency Degradation ($\Delta\eta$): It is helpful to introduce the concept of efficiency degradation, $\Delta\eta$. This parameter describes the proportional loss in efficiency due to a proximate spurious mode. It neglects the reduction of efficiency that can occur from losses in the optimum resonant mode regardless of spurious-mode interactions. We define it thus

$$\Delta\eta = 1 - \frac{\eta_2}{\eta_1} \tag{20}$$

where η_1 is the efficiency calculated from the single-branch model, and η_2 is the efficiency calculated from the two-branch model. It is worth noting that $\Delta\eta$, like η_2, is a function of L_1, L_2, C_1, C_2, R_1, R_2, N_1, N_2, C_{out}, ω, and R_L. It is useful to perform a series of substitutions so that efficiency is written in terms of resonant frequencies

$$\omega = \omega_1;\ \ \omega_1 = \frac{1}{\sqrt{L_1 C_1}};\ \ \omega_2 = \frac{1}{\sqrt{L_2 C_2}};$$
$$\zeta_1 = \sqrt{\frac{L_1}{C_1}};\ \zeta_2 = \sqrt{\frac{L_2}{C_2}} \tag{21}$$

where ω_1 and ω_2 are the resonant frequencies of the optimum and spurious mode, respectively, and ζ_1 and ζ_2 are the magnitude of the reactance of L_1 and L_2 (or C_1 and C_2), respectively, at the relevant resonant frequency. These substitutions eliminate L_1, L_2, C_1, and C_2 from (20) and also eliminates ζ_1, therefore simplifying the (still long) expression.

C. Sensitivity Analysis

Owing to the complexity of the efficiency degradation mechanism in a PT, it is not easy to determine which equivalent circuit parameters have a significant effect. We therefore perform a sensitivity analysis to isolate the relevant parameters.

1) One Factor at a Time: The "one-factor-at-a-time" is the simplest type of sensitivity analysis to perform and to understand. The results of this analysis will help to show the general trends that each of the circuit parameters have on efficiency degradation. While the results of this analysis are focused around one specific PT (T1-13 in this case), similar results would be achieved for other PT topologies, noting the similarity between equivalent parameters.

The analysis is performed with the exemplar PT parameter set in Table II. However, the T1-13 PT has low efficiency degradation owing to the significant frequency difference between its optimum (radial) mode and any spurious mode. However, as described in [7] spurious modes are typically not considered in the design process and therefore, an optimized frequency difference is not likely to be true of initial designs. Subsequent sensitivity analyses will therefore be performed on a modified set of parameters, based on the T1-13, which brings ω_2 closer to ω_1 while maintaining all other parameters. This PT model, which we will term T1*, has the parameters given in Table II. The new design improves the viewability of the sensitivity analysis and represents a realistic early PT design. At matched load and optimum resonant frequency, this modification increases the efficiency degradation from –0.04% to 1.46% (for single-branch efficiency η_1 of 97.4%).

To perform the sensitivity analysis, a range of parameters to study is required. Each of the parameters will be varied through the range $x_\mathrm{n}/100 \leq x \leq 100x_\mathrm{n}$, where x is the parameter and x_n is its nominal value from Table II. This allows the analysis to cover a wide range of potential devices. The only exception is the turns ratios (N_1, N_2), which will only be varied in the range $N_\mathrm{n}/10 \leq N \leq 10N_\mathrm{n}$ because the turns ratio typically correlates linearly to the geometry, which is physically constrained.

a) Initial study on exemplar PT, T1-13:

b) Study on modified PT, T1*: Each curve in Fig. 9 demonstrates the effect of varying a single parameter while keeping the other parameters at their nominal value. As shown in Fig. 9, ζ_2 has the greatest effect on efficiency degradation. As ζ_2 decreases from its nominal value, the efficiency degradation rapidly increases. Each of the other parameters has minimal effect on the efficiency degradation across its full range of variation. However, as discussed above, the overall low efficiency degradation is unrealistic for early designs (such as those generated using [7]), due to the large frequency difference between modes. Nevertheless, from the initial analysis, we can see that ζ_2 is a vital design parameter in ensuring low efficiency degradation.

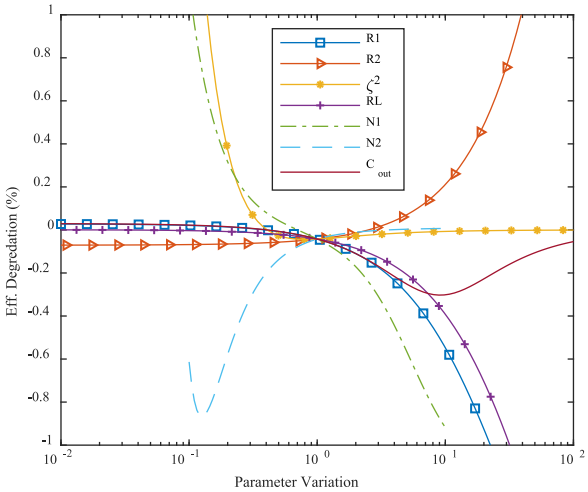

Fig. 9. Sensitivity analysis on the influence of parameter value on the efficiency degradation of a nominal T1-13 PT.

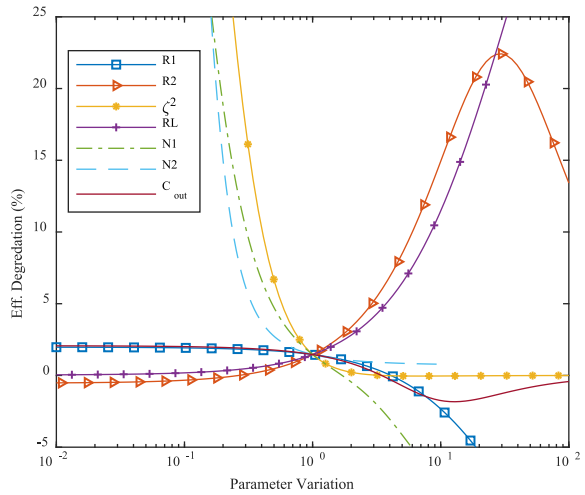

Fig. 10. Sensitivity analysis on the influence of parameter value on the efficiency degradation of the T1* PT.

Fig. 10 shows the same analysis performed on the modified model, T1*. Comparing Fig. 10 to Fig. 9 shows that each of the parameters has an increased effect on the efficiency degradation when the spurious mode is closer to the optimum mode. ζ_2 remains the parameter with the largest effect on efficiency degradation, again highlighting its importance in design. N_2, R_L N_1, and R_2 all have significant effects on the efficiency degradation, with proximity of the modes determining how impactful the parameter is. For this case study, R_1 and C_out have negligible effect on efficiency degradation compared to the other parameters. It should be noted that negative efficiency degradation, means an efficiency increase caused by the spurious mode. However, using (8) it can be concluded that increasing these parameters decreases optimum mode efficiency and so should typically be avoided.

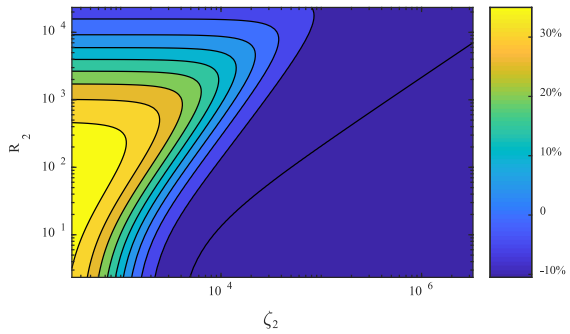

Fig. 11. Contour plot of efficiency degradation with changes in ζ_2 and R_2.

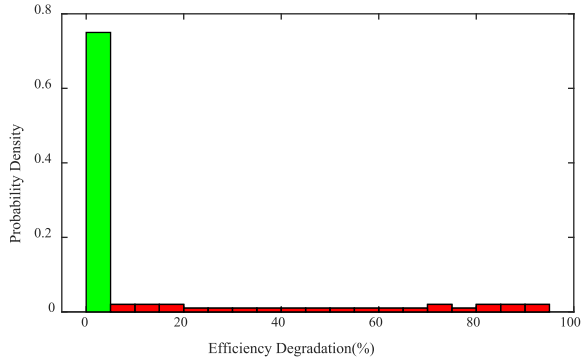

Fig. 12. Probability density plot for $R_2 = 5.4\ \Omega$, the green bar highlighting the desired (<5% $\Delta\eta$) specification.

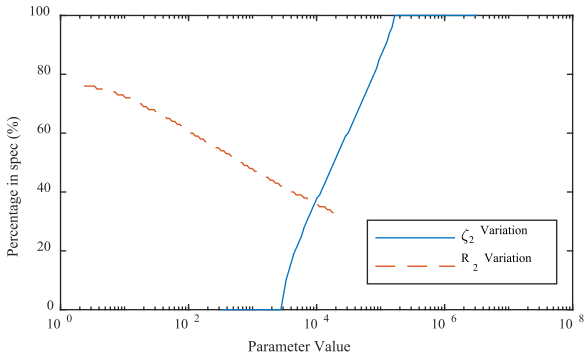

Fig. 13. Percentage of datapoints in specification against variation in each parameter's values.

The effect R_2 has on the efficiency degradation is interesting. Initially, as one would expect, increasing R_2 increases the efficiency degradation due to higher I^2R losses. However, beyond a certain value (30 times nominal), the efficiency degradation peaks, thereafter falling with increased R_2. This effect is due to reduced power flow in the spurious mode, therefore, if $R_2 = \infty$, there is no power through the spurious mode and so no efficiency degradation. However, as damping in PTs is largely due to mechanical losses, common to all modes, higher damping in the spurious mode typically results in higher damping in the optimum mode [17]. Therefore, while increasing the damping (i.e., R_2) in the PT may minimize efficiency degradation, it will typically cause a decrease in the optimum mode efficiency of the PT (due to increases in R_1) and thus degrade performance. However, if a designer could increase the damping in a specific mode without affecting the optimum mode, this would be a good option for improving the efficiency degradation in the device.

2) Parametric Sweep: While studying variations of a single parameter gives useful insight into how the efficiency degradation of a specific PT is affected by each parameter in isolation, the results of a "one-factor-at-a-time" analysis are dependent on the device studied. To study multiple parameters simultaneously, a parametric sweep based sensitivity analysis is performed. For this analysis, all parameters are varied in a 7-D space with each dimension having the same range of variation as the previous analysis, which was derived from the T1-13 PT (see Table II).

To visualize the results, each parameter (dimension) is varied in turn and the 6-D space extracted. We then define a good device, as one that achieves an efficiency degradation of less than 5%. The proportion of good devices in this space is calculated. Graphical plots are then produced showing the trend in the proportion of good devices with the parameter at hand.

To further describe this type of analysis, a simplified scenario is shown with only two input variables: ζ_2 and R_2. The efficiency degradation will be analyzed for each variation of both parameters. The T1* PT will be used for the remaining parameters, as given in Table II. First, these data can be visualized on a 3-D graph, as only two parameters are considered. This is shown in Fig. 11.

Although with greater than two input variables, such as in our analysis, it is impractical to visualize the data on a single graph.

To overcome this, first, for each variation of a parameter's value a probability density plot can be produced, showing the likelihood of achieving various levels of efficiency degradation. An example plot is shown for $R_2 = 5.4\Omega$.

From Fig. 12, we calculate that 75% of devices are within the specification (<5% $\Delta\eta$) when $R_2 = 5.4\Omega$. This process is then repeated for all values of the said parameter, and a graph of percentage of devices in specification against the variation in the parameter value can be produced, as shown in Fig. 13. This process is then repeated for the remaining parameter(s), as also shown in Fig. 13.

From Fig. 13, we can see a similar general trend as was visible in the 3-D plot in Fig. 11, with a positive and a negative correlation observed for ζ_2 and R_2, respectively. It should be noted that more subtle trends are lost in this analysis, such as $\Delta\eta$ improving with very large R_2 values.

To perform this analysis on a PT, several changes need to be made from the "one-factor-at-a-time" analysis, although, the range of parameter variation will be kept the same. First, as there is no longer a nominal device, it is important that all results are indepedent of the chosen optimum mode resonant frequency. Therefore, C_{out} will be considered as an impedance ($X_{C_{\text{out}}} = -1/\omega C_{\text{out}}$), to ensure matched load conditions do not affect the results. In this case, $X_{C_{\text{out}}}$ will be varied from 13.2 Ω to 132 kΩ. Second, the spurious mode resonant frequency is set as $\omega_2 = 0.9\omega_1$ and $\omega_2 = 1.1\omega_1$. The close proximity of the modes to the optimum mode, will accentuate the affect each parameter has and, using multiple spurious resonant frequencies, highlights

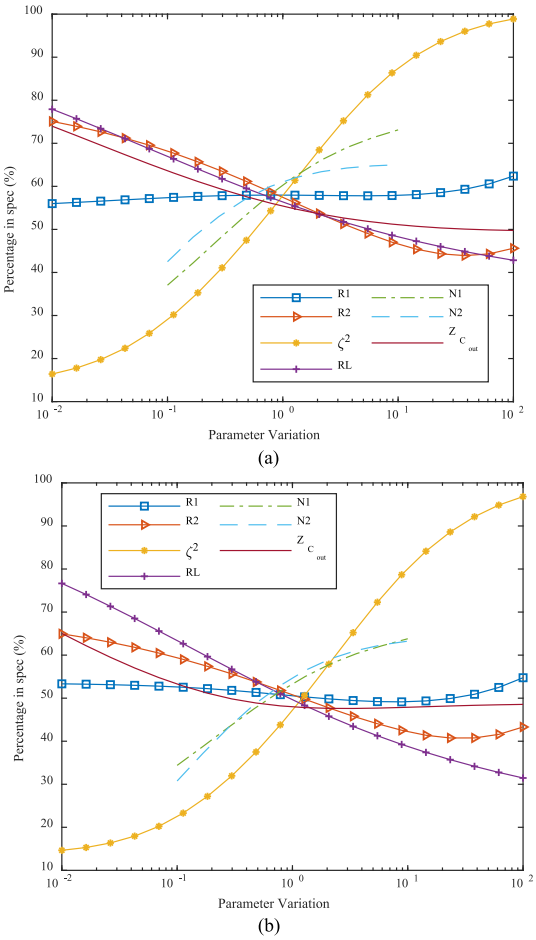

Fig. 14. Parametric sweep based sensitivity analysis. (a) $\omega_2 = 0.9\,\omega_1$. (b) $\omega_2 = 1.1\,\omega_1$.

the differences between modes occurring at frequencies either side of the optimum mode resonance. The results of the parametric sweep sensitivity analysis are presented in Fig. 14.

Fig. 14 shows that all parameters have some influence on the proportion of good devices and hence the efficiency degradation. However, ζ_2 has the greatest effect on the number of good devices, with a change of up to 82.5 percentage points (from worst to best case ζ_2 value) in the percentage of devices exhibiting $<5\%$ efficiency degradation. This analysis also highlights the impact the load resistor R_L has on the proportion of acceptable devices. A change of up to 45.2 percentage points is observed across the parameter range.

In a similar way to R_L, increases in R_2 and C_{out} cause a decrease in the proportion of good devices. Conversely, N_1 and N_2 have a similar impact on the proportion of good devices, each with an increase of up to 36 percentage points across the parameter range. R_1 has a negligible effect when compared to the other parameters.

III. PT Design for Minimal Efficiency Degradation

From the previous analyses, a few parameters have been highlighted as vital for low efficiency degradation. Most notably, these include frequency difference and ζ_2. Previous analyses have also shown that both variables have a negative correlation with efficiency degradation. From the parametric sweep sensitivity analysis, it was also found that for ζ_2 values greater than $\sim$18 MΩ, all PTs have minimal efficiency degradation, irrespective of the other parameter values (given they are in the range used for this analysis). This is useful from a design perspective, as efficiency loss from spurious modes can be negated by careful design of only a single parameter, especially as ζ_2 has no impact on optimum mode performance. However, the critical value of ζ_2 (that required 100% of devices tested to exhibit $<5\%$ $\Delta\eta$) from the parametric sweep sensitivity analysis is at least two orders of magnitude greater than that exhibited by the T1-13 PT, and such a large value may be unachievable.

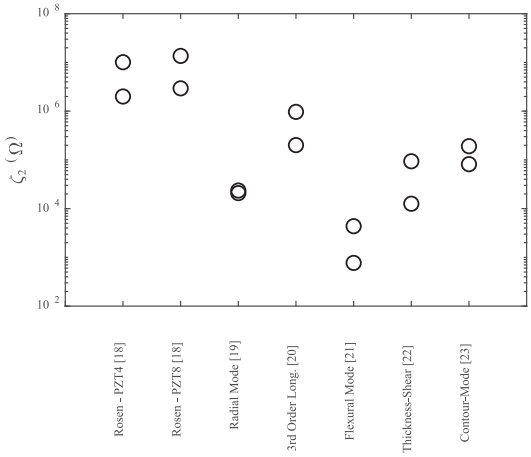

Fig. 15. Typical ζ_2 values exhibited by several different PT topologies.

A. Typical ζ_2 Values Achieved by PTs

The following section will analyze the typical ζ_2 values that are typically achieved in various PTs topologies. This will help to give some context to ζ_2 values that are required to avoid minimal spurious mode interaction for all PTs.

To determine typically achievable values of ζ_2, a COMSOL simulation study was performed on various different PT topologies [18]–[23]. For each PT examined, an eigenfrequency study was performed, allowing the resonant frequencies to be extracted. The impedance of each PT at frequencies surrounding the two nearest spurious modes to the optimum mode were simulated, and ζ_2 extracted using a method presented by Forrester *et al.* [24]. The results of this analysis are presented in Fig. 15.

As shown in Fig. 15, there is significant variation in ζ_2 exhibited across the range of PT topologies. The bar shaped PTs (Rosen and third-order longitudinal) exhibit very large ζ_2, so large that these PTs should have minimal efficiency degradation irrespective of the other equivalent parameters. However, the other PT topologies exhibit significantly smaller ζ_2 values. Fig. 15 also shows that using a harder PZT, such as PZT8, leads to larger ζ_2 values than the softer PZT4. Importantly, this analysis has also shown that most PTs, even if made from PZT8, will not achieve a ζ_2 greater than the $\sim$18 MΩ that is required to ensure minimal $\Delta\eta$.

However, Fig. 14 shows that changing the frequency of the spurious mode changes the percentage of devices exhibiting less than 5% efficiency degradation for the same ζ_2 value. This is further confirmed by the "one-factor-at-a-time" analyses, as for the same ζ_2 value, different levels of efficiency degradation were achieved at different $\Delta\omega$ values. Therefore, the critical value of ζ_2, at which all PTs analyzed had <5% efficiency degradation, will change with proximity of the spurious mode to the optimum mode. Furthermore, with greater frequency difference, the critical value of ζ_2 will be smaller and more achievable.

B. Analyzing the Influence of Frequency Separation and ζ_2 on the Percentage of Good Devices

Previous analyses have proven that mode proximity and a large ζ_2 value are key factors in ensuring low efficiency degradation. Therefore, the following analysis will focus on analyzing the combined impact these two parameters have on the efficiency degradation. This will be extended by analyzing various scenarios, which constrain the other equivalent parameters. This will provide insight into the optimum frequency separation for a given ζ_2, informing PT design decisions.

The relationship between frequency separation ($\Delta\omega = (\omega_2 - \omega_1)/\omega_1$), ζ_2 and the percentage of devices achieving <5% efficiency degradation will be analyzed. Similar to the parametric sweep sensitivity analysis, all parameters will be independently varied in a 7-D space. However, in this analysis, the spurious mode resonant frequency will also be included in the variation, with load being matched to the output capacitance, and therefore not independently varied. The PT will be driven at the optimum mode resonant frequency and all other parameters varied in the same way as the previous parametric sweep analysis. The percentage of good devices (<5% $\Delta\eta$) for variations in ζ_2 and $\Delta\omega$ will be extracted and plotted, using the same method as in the parametric sweep analysis. The range of variation for all parameters is kept the same as in previous sensitivity analyses, with $\Delta\omega$ varied between $-0.75 < \Delta\omega < 0.75$ by changing ω_2, with ω_1 fixed at 100 kHz (although, choice has no impact on the results). A contour plot of $\Delta\omega$, ζ_2, and percentage of good (exhibiting <5% $\Delta\eta$) devices is shown in Fig. 16.

As theorized, the results in Fig. 16 show that the values of ζ_2 required to ensure all devices have <5% $\Delta\eta$ decreases with spurious mode proximity to the optimum mode. However, even with a frequency difference of –0.75, ζ_2 values in excess of 1 MΩ are required for 100% of devices to be classed as good, with only 1.25% of combinations (of ζ_2 and $\Delta\omega$) leading to 100% of devices being good. The asymmetry in the results should also be noted. As a result, for the same value of ζ_2, a spurious resonance would require a greater frequency difference if it occurs at a frequency greater than the optimum mode, compared to a mode occurring below ω_1.

C. Parameter Range Effect on Required ζ_2 and $\Delta\omega$

Several different stipulations will be applied to the range of parameter variation in order to provide insight into realistic requirements for ζ_2 and $\Delta\omega$.

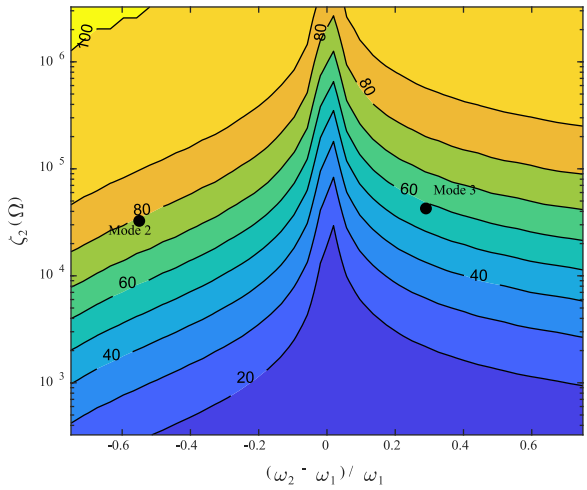

Fig. 16. Contour plot of the percentage of good devices, against ζ_2 and $\Delta\omega$. Modes 2 and 3, corresponding to the first and second spurious modes, respectively, of the T1-13 PT.

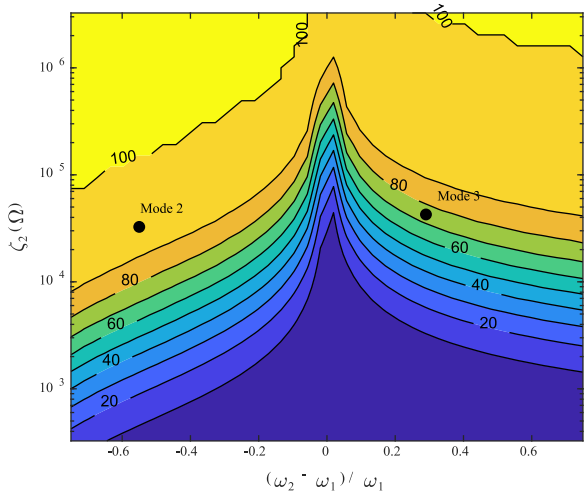

Fig. 17. Contour plot of the percentage of good devices against ζ_2 and $\Delta\omega$, with the parameter space of the other parameters reduced. Modes 2 and 3, corresponding to the first and second spurious modes, respectively, of the T1-13 PT.

1) Reducing Parameter Range: The wide range of parameter variation used throughout the previous analyses ensures that most potential PT designs are included. However, typically PT designs will have parameters similar to the nominal T1-13 PT. Therefore, removing some of the more extreme parameter variations will give results that are more relevant to typical PT designs. A similar analysis to that in Fig. 16 will be performed; however, the range of parameter variation will be $x_n/10 \leq x \leq 10x_n$, where x is the parameter and x_n is its nominal value from Table II and $N_n/5 \leq N \leq 5N_n$ for the turns ratios (N_1 and N_2). Again, $\Delta\omega$ is varied, by changing ω_2, between $-0.75 < \Delta\omega < 0.75$, ω_1 is again assumed to be 100 kHz. The results of this analysis are shown in Fig. 17.

Fig. 17 shows that reducing the range of parameter variation greatly reduces the required ζ_2 values for 100% of devices to exhibit <5% $\Delta\eta$, with 16.3% of combinations (of ζ_2 and $\Delta\omega$)

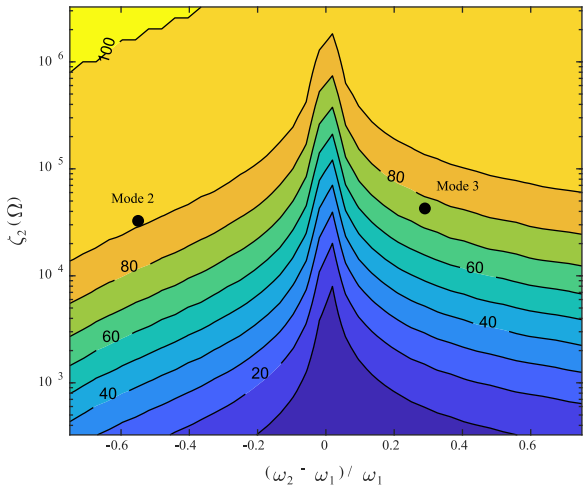

Fig. 18. Contour plot of the percentage of good devices against ζ_2 and $\Delta\omega$, with the damping resistances R_1 and R_2 less than 50 and 500 Ω, respectively. Modes 2 and 3, corresponding to the first and second spurious modes, respectively, of the T1-13 PT.

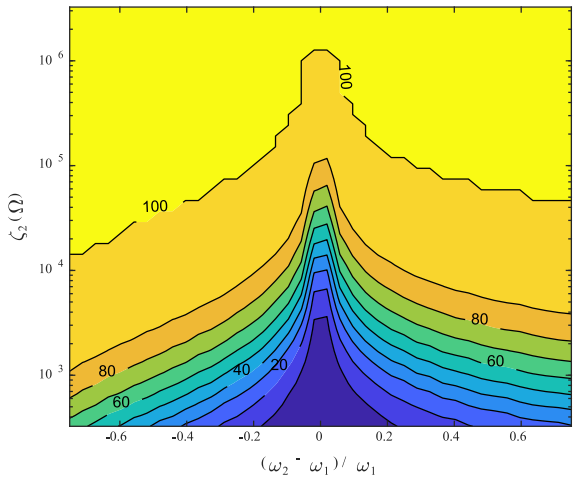

Fig. 19. Contour plot of the percentage of good devices against ζ_2 and $\Delta\omega$, with optimum mode efficiency η_1 greater than 80%, load fixed at 25 Ω, and the damping resistance R_2 no larger than $15R_1$.

leading to 100% of devices being good. However, this graph also shows that for small $|\Delta\omega|$ and ζ_2 values, a smaller percentage of devices have <5% $\Delta\eta$. This highlights that while the extreme parameter variations in some cases greatly increase $\Delta\eta$, in other cases these extreme variations can allow a PT to be have <5% $\Delta\eta$, even when exhibiting small $\Delta\omega$ and ζ_2. However, $\Delta\omega$ and ζ_2 values required for 80%+ of devices to be good, has greatly reduced.

2) Lower Damping: Typically, a PT will be designed for high optimum mode efficiency. As described earlier (Section II-B1), minimizing R_1 is vital for high optimum mode efficiency. R_1 values of <50 Ω are typical in PZT-based devices and as a result, 90%+ efficiency can be easily achieved irrespective of the other equivalent circuit parameters, when operated at the matched load. Also discussed previously, spurious mode damping is linked to optimum mode damping and so, if a PT is designed for high optimum mode efficiency (low R_1), then R_2 is also typically, relatively small. Again, these stipulations will be analyzed. The range of parameter variation will be the same as in Fig. 16. However, devices exhibiting $R_1 > 50\Omega$ and/or $R_2 > 500\Omega$ will be excluded from the analysis. It should be noted that 50 Ω was chosen by assuming 95% or better efficiency is desired in the optimum mode (if it is assumed $C_{\text{out}} = 0$, $R_L = 1$ kΩ and $N_1 = 1$) and 500 Ω was chosen noting the ratio of R_1/R_2 in the T1-13 PT. It should be noted that $X_{C_{\text{out}}}$, R_L, and N_1 are all still varied through the same range as was used in Fig. 16; the assumptions above were used exclusively to determine the desired range of R_1 and R_2. The results of this analysis are shown in Fig. 18.

The results in Fig. 18 are similar those in Fig. 17, with lower ζ_2 values leading to a higher percentage of devices achieving <5% $\Delta\eta$ for the same $\Delta\omega$, compared to Fig. 16. However, again for small $|\Delta\omega|$ and small ζ_2 values, a slightly lower percentage of good devices is achieved, compared to Fig. 16. Fig. 18 also shows that reducing R_1 and R_2 makes achieving <5% $\Delta\eta$ easier.

3) Design Case Study—5-V, 1-W Output: A potential application for PTs is in low power, resonant converters, such as those used for charging mobile phones, tablets, or laptops. In these applications typically a 5-V output is required, providing 1 W to the load, leading to a load resistance of 25 Ω. Ideally, the transformer should have high efficiency, as losses across the switching and rectification elements will also reduce the overall system efficiency, which is beyond the scope of this analysis. Therefore, in this analysis, the PT will be designed to achieve an optimum mode efficiency greater than 80%. Given these stipulations, an analysis can be performed to determine desired ζ_2 and $\Delta\omega$ values for minimal $\Delta\eta$.

For this analysis, all parameters will be varied through the same range as in Fig. 16 with the load fixed at 25 Ω. All combinations of parameters that lead to an optimum mode efficiency of <80% will be removed from the analysis. Noting the ratio of R_1/R_2 in the T1-13 PT, devices exhibiting R_2 values $> 15R_1$ were also removed from the analysis. It should be noted that, as the input voltage is not given in this scenario, the desired value of N_1 to achieve 5-V output is unknown. Its value is therefore varied through the full range as was used in Fig. 16. The results of this analysis are presented in Fig. 19.

As is shown in Fig. 19, the required ζ_2 value to achieve <5% $\Delta\eta$ in 100% of devices for a given $\Delta\omega$ is greatly reduced in this scenario. As in previous figures, for small ζ_2 and $|\Delta\omega|$ values, fewer devices achieve <5% $\Delta\eta$ than in Fig. 16. However, observing the ζ_2 values presented in Fig. 15, in most cases a frequency difference of –0.37> $\Delta\omega$ and/or $\Delta\omega > 0.56$ will ensure that, as long as the other equivalent circuit values are within the relevant ranges, the PT should exhibit minimal efficiency degradation.

However, as with all of the results published here, if a PT exhibits ζ_2 and $\Delta\omega$ values that lead to <100% of devices achieving <5% $\Delta\eta$, then it is still possible that a specific PT will have minimal $\Delta\eta$. Therefore, the results presented should be used as a guideline for design and if accurate estimations of

TABLE III
EQUIVALENT CIRCUIT COMPONENTS FOR MODE OCCURRING AT A FREQUENCY ABOVE THE OPTIMUM IN THE T1-13 PT

	R_3	$\omega_3/2\pi$	ζ_3	N_3
T1-13	234.9 Ω	154.7 kHz	42,637 Ω	1.31

TABLE IV
ζ AND $\Delta\omega$ VALUES FOR THE TWO SPURIOUS MODES OCCURRING CLOSEST (IN TERMS OF FREQUENCY) TO THE OPTIMUM MODE

	Mode 2	Mode 3
ζ	32.6 kΩ	42.6 kΩ
$\Delta\omega$	-0.55	0.29

TABLE V
ESTIMATED PERCENTAGE CHANCE OF ACHIEVING $<5\%$ $\Delta\eta$ FOR BOTH MODES FROM THE CONTOUR PLOTS PREVIOUSLY PRESENTED IN THE RESPECTIVE FIGURES

	Mode 2	Mode 3
Fig. 16	80.8 %	59.4 %
Fig. 17	97.9 %	77.0 %
Fig. 18	92.2 %	77.8 %

the efficiency degradation in the PT are required, then they can be generated using the equations presented earlier.

IV. EXPERIMENTAL VALIDATION

To validate the findings, the T1-13 PT will have its efficiency measured at the optimum frequency. The input impedance spectrum for this device is shown in Fig. 1. The efficiency is compared to predictions made using the equivalent circuit parameters presented in Table II and the various contour plots (Figs. 16–18). It is important to note that it is not possible to directly measure efficiency degradation (as the modes are inseparable). The single-branch efficiency (η_1) was therefore estimated from the equivalent circuit parameters. A sinusoidal voltage was supplied to the PT and the input power, output power and efficiency were measured using a Yokogawa PX-8000 power oscilloscope. Using the estimated single-branch efficiency and measured efficiency, an estimate of efficiency degradation can be made. For this analysis, a load of 1 kΩ (approx. matched) was used. Also, in this PT there are two offending spurious modes, which will be analyzed separately.

First, the equivalent circuit parameters of the third most significant mode (second spurious mode in Fig. 1) are extracted and shown in Table III. Efficiency degradation from this mode can be found by using R_3, ω_3, ζ_3, and N_3 in place of R_2, ω_2, ζ_2, and N_2.

The ζ and $\Delta\omega$ values for the first and second spurious modes (see Fig. 1) are shown in Table IV.

In the contour plots (Figs. 16–18), the percentage of good devices ($<5\%$ $\Delta\eta$) with the ζ_2 and $\Delta\omega$ values from Table IV can be found. They are labeled on each figure and summarized in Table V.

As Table V summarizes, both modes exhibit high percentage chances of achieving $<5\%$ $\Delta\eta$, with a maximum of 97.9% and 77.8% for first and second spurious modes, respectively. This suggests that both first and second spurious modes are not guaranteed to have no influence on optimum mode performance. However, with these modes achieving a high percentage chance of $<5\%$ $\Delta\eta$ in Figs. 16–18, it is highly likely they would have no influence on optimum mode performance, especially considering they exhibit a high turns ratio and low damping compared to the maximum 500 Ω used in the analysis shown in Fig. 18.

For validation, the efficiency degradation of the PT is measured. The optimum mode efficiency was estimated using the equivalent circuit values in Table II and using (8). Using this value and the experimentally measured efficiency, the efficiency degradation is found.

For this PT and a 1-kΩ load, the optimum mode efficiency is calculated at 97.3%. The efficiency is then experimentally measured as 96.9%. Using (20), the efficiency degradation is 0.4%. Therefore, confirming the PT does exhibit $<5\%$ efficiency degradation from both spurious modes.

V. DISCUSSION

This article has highlighted the importance of optimizing certain parameters at the design stage. As a result, designing a PT to exhibit large ζ_2 is vital, as this is the most influential parameter for minimizing efficiency degradation while having a negligible effect on optimum mode performance. Second, decreasing damping in both the optimal and spurious modes is important for high efficiency. Both are typically determined by the piezoelectric material chosen, the electrode material chosen, and the construction of the PT. Finally, increasing the spurious mode turns ratio also has a beneficial effect on $\Delta\eta$ while not affecting optimum mode performance. However, designing this parameter is difficult, as it requires knowledge of the type of spurious mode and how geometry or material changes affect its parameters.

It can be seen that efficiency loss from spurious modes can be minimized though careful design of the spurious mode resonant frequencies and ζ_2. It has also been shown that the required ζ_2 can be reduced through careful design of the other equivalent circuit values. Therefore, the analysis in this article provides designers with a method of appraising designs and, if required, provides information regarding potential design improvements.

It should also be noted that while the analysis here looks at the required components and design to achieve less than 5% efficiency degradation, it does not analyze how far below or above 5% efficiency degradation represents a good or bad design. Readers will be able to reproduce the graphs for any desired efficiency degradation or nominal PT parameters using the presented equations.

The presence of spurious modes also causes an unwanted reduction in the output voltage. Therefore, even with appropriate optimum mode design, a PT may not supply the intended output voltage. However, improvements to efficiency degradation by adjusting spurious mode parameters (ω_2, R_2, N_2, and ζ_2), minimizes the output voltage reduction, further demonstrating the importance of appropriate design for these parameters. R_1 and

C_{out} have a complicated relationship with voltage degradation and so decreasing their value (to decrease $\Delta\eta$) can increase or decrease voltage degradation depending on other parameters. Increasing the optimum mode turns ratio (N_1) to decrease $\Delta\eta$ causes voltage degradation to increase and therefore should be avoided. However, in T1-13 PT the voltage degradation was $<1\%$, and so in most cases, voltage degradation is unlikely to be an issue.

Due to the number of variables that influence the efficiency degradation and the wide range of potential variation in these parameters, there will be cases where a parameter is outside the presented range of variation. The results of this analysis should be used as a guideline for appropriate design with a view to produce an exact specification following circuit and finite element analysis. The parameters of a PT design should be carefully analyzed using the equations presented in this article to calculate the efficiency degradation and the required ζ_2.

Spurious modes will typically occur at frequencies both above and below the optimum mode frequency. However, the analysis in this article has primarily considered interaction with a single spurious mode. We assume that each spurious mode can be considered and analyzed separately, which is likely in practice.

VI. Conclusion

An analysis of the impact of spurious modes on the efficiency of PTs was presented. Circuit analysis was performed on PT models with both a single resonant branch and with two resonant branches to generate equations for the efficiency of each model. Multiple sensitivity analyses were then performed and ζ_2 was highlighted as a critical design consideration. The value of ζ_2 required for minimal efficiency degradation in all devices was found. Furthermore, analysis of the combined effect of ζ_2 and $\Delta\omega$ was performed. This analysis was repeated with the parameter space of all other materials restricted in various scenarios. Results of this analysis provide a method of estimating the extent to which a spurious mode will degrade efficiency and consequently, through the results of the sensitivity analyses, provide a method for improving PT designs.

References

[1] S. J. Huang, T. S. Lee, and P. Y. Lin, "Application of piezoelectric-transformer-based resonant circuits for AC LED lighting-driven systems with frequency-tracking techniques," *IEEE Trans. Ind. Electron.*, vol. 61, no. 12, pp. 6700–6709, Dec. 2014.

[2] E. Wells, "Comparing magnetic and piezoelectric transformer approaches in CCFL applications," Texas Instruments Incorporated, Dallas, TX, USA, Application Notes, p. 7, 2002.

[3] M. Ekhtiari, T. G. Zsurzsan, M. A. E. Andersen, and Z. Zhang, "Optimum phase shift in the self-oscillating loop for piezoelectric-transformer-based power converters," *IEEE Trans. Power Electron.*, vol. 33, no. 9, pp. 8101–8109, Sep. 2018.

[4] T. Martinez, G. Pillonnet, and F. Costa, "A 15-mV inductor-less start-up converter using a piezoelectric transformer for energy harvesting applications," *IEEE Trans. Power Electron.*, vol. 33, no. 3, pp. 2241–2253, Mar. 2018.

[5] A. Camarda, M. Tartagni, and A. Romani, "A $-$ 8 mV/ $+$15 mV double polarity piezoelectric transformer-based step-up oscillator for energy harvesting applications," *IEEE Trans. Circuits Syst. I, Reg. Papers*, vol. 65, no. 4, pp. 1454–1467, Apr. 2018.

[6] K. Suzuki, K. Adachi, Y. Shibamata, and T. Suzuki, "Structure of 100 W high-efficiency piezoelectric transformer for applications in power electronics," *Jpn. J. Appl. Phys.*, vol. 55, no. 8, Jul. 2016, Art. no. 086702.

[7] J. Forrester, J. N. Davidson, M. P. Foster, E. L. Horsley, and D. A. Stone, "Automated design tools for piezoelectric transformer-based power supplies," *J. Eng.*, vol. 2019, no. 17, pp. 4163–4166, 2019.

[8] M. P. Foster, J. N. Davidson, E. L. Horsley, and D. A. Stone, "Critical design criterion for achieving zero voltage switching in inductorless half-bridge-driven piezoelectric-transformer-based power supplies," *IEEE Trans. Power Electron.*, vol. 31, no. 7, pp. 5057–5066, Jul. 2016.

[9] A. M. Flynn and S. R. Sanders, "Fundamental limits on energy transfer and circuit considerations for piezoelectric transformers," *IEEE Trans. Power Electron.*, vol. 17, no. 1, pp. 8–14, Jan. 2002.

[10] K. Brebøl, "Piezoelectric transformer," U.S. Patent, 6 707 235 B1, Mar. 16, 2004.

[11] O. Ohnishi, H. Kishie, A. Iwamoto, Y. Sasaki, T. Zaitsu, and T. Inoue, "Piezoelectric ceramic transformer operating in thickness extensional vibration mode for power supply," in *Proc. IEEE Ultrason. Symp.*, 1992, vol. 1, pp. 483–488.

[12] T. Ikeda, *Fundamentals of Piezoelectricity*. New York, NY, USA: Oxford Univ. Press, 1990.

[13] R. Prieto, M. Sanz, J. A. Cobos, P. Alou, O. Garcia, and J. Uceda, "Design considerations of multi-layer piezoelectric transformers," in *Proc. 16th Annu. IEEE Appl. Power Electron. Conf. Expo.*, 2001, vol. 2, pp. 1258–1263.

[14] M. Sanz, P. Alou, J. A. Oliver, R. Prieto, J. A. Cobos, and J. Uceda, "Interleaving of electrodes in piezoelectric transformers," in *Proc. IEEE 33rd Annu. IEEE Power Electron. Spec. Conf.*, 2002, vol. 2, pp. 567–572.

[15] G. Ivensky, I. Zafrany, and S. Ben-Yaakov, "Generic operational characteristics of piezoelectric transformers," *IEEE Trans. Power Electron.*, vol. 17, no. 6, pp. 1049–1057, Nov. 2002.

[16] R.-L. Lin, "Piezoelectric transformer characterization and application of electronic ballast," Ph.D. dissertation, Dept. Elect. Comput. Eng., Virginia Polytech. Inst. State Univ., Blacksburg, VA, USA, Nov. 2001.

[17] V. Loyau, Y. P. Liu, and F. Costa, "Analyses of the heat dissipated by losses in a piezoelectric transformer," *IEEE Trans. Ultrason., Ferroelect., Freq. Control*, vol. 56, no. 8, pp. 1745–1752, Aug. 2009.

[18] Megacera Inc., "PT291C3 specification sheet," Oct. 15, 2001. [Online]. Available: http://mmech.com/images/stories/Standard_Products/Transformers/High_Voltage/PT291C3_Specification_Sheet.pdf

[19] Micromechatronics Inc., "Transoner data sheet," May 24, 2005. [Online]. Available: http://mmech.com/images/stories/Standard_Products/Transformers/Step_Down/Datasheet_of_T1-noniso-6_-_MMech.pdf

[20] S. Kawashima *et al.*, "Third order longitudinal mode piezoelectric ceramic transformer and its application to high-voltage power inverter," in *Proc. IEEE Ultrason. Symp.*, 1994, vol. 1, pp. 525–530.

[21] Y. Huang, Z. Miao, X. Chen, and W. Huang, "A verification and parametric analysis of an analytical model of a flexural vibration mode piezoelectric transformer," *IEEE Trans. Ultrason., Ferroelect., Freq. Control*, vol. 59, no. 12, pp. 2731–2741, Dec. 2012.

[22] J. Du, J. Hu, and K.-J. Tseng, "High-power, multioutput piezoelectric transformers operating at the thickness-shear vibration mode," *IEEE Trans. Ultrason., Ferroelect., Freq. Control*, vol. 51, no. 5, pp. 502–509, May 2004.

[23] J. Yoo, K. Yoon, Y. Lee, S. Suh, J. Kim, and C. Yoo, "Electrical characteristics of the contour-vibration-mode piezoelectric transformer with ring/dot electrode area ratio," *Jpn. J. Appl. Phys.*, vol. 39, no. 5A, p. 2680, pp. 2680–2684, May 2000.

[24] J. Forrester *et al.*, "Equivalent circuit parameter extraction of low-capacitance high-damping PTs," *Electron. Lett.*, vol. 56, pp. 347–350, Mar. 2020.

Jack Forrester received the M.Eng. degree in electrical and electronic engineering, in 2017, from the University of Sheffield, Sheffield, U.K., where he is currently working toward the Ph.D. degree in the area of piezoelectric transformer based power converters, with a focus on transformer design and characterization.

Jonathan Neil Davidson received the M.Eng. degree in electronic engineering and Ph.D. degree in thermal modeling and management from the University of Sheffield, Sheffield, U.K., in 2010 and 2015, respectively.

In 2015, he joined the University of Sheffield as a member of Academic Staff. His research interests include the thermal modeling and management of power electronics, piezoelectric transformers, resonant converters, electrical metrology in sewerage systems, and plasma-generating electronics.

Martin P. Foster received the B.Eng. degree in electronic and electrical engineering, the M.Sc. (Eng.) degree in control systems, and the Ph.D. degree in power electronics from the University of Sheffield, Sheffield, U.K., in 1998, 2000, and 2003, respectively.

In 2003, he became a Member of Academic Staff specializing in power electronic systems at the University of Sheffield, where he became Senior Lecturer in 2010, Reader in 2014, and Professor of energy storage and conversion in 2017. His research interests include the modeling and control of switching power converters, resonant power supplies, multilevel converters, energy storage management systems, piezoelectric transformers, and power electronic packaging and thermal management.

David A. Stone received the B.Eng. degree in electronic engineering from the University of Sheffield, Sheffield, U.K., in 1984, and the Ph.D. degree from Liverpool University, Liverpool, U.K., in 1989.

He then joined the Electrical Machines and Drives Group, University of Sheffield, where he is currently a Professor of electrical engineering. His research interests include battery management, energy storage and conversion, energy utilization, and power electronic applications including dc–dc and motor drive systems.